To cite this version:

Tisserant, Gwendoline and Gillion, Julie and Lannelongue, Jérémy and Fattah, Zahra and Garrigue, Patrick and Roche, Jérôme and Zigah, Dodzi and Kuhn, Alexander and Bouffier, Laurent *Single-Step Screening of the Potential Dependence of Metal Layer Morphologies along Bipolar Electrodes.* (2015) ChemElectroChem, 3 (3). 387-391. ISSN 2196-0216

Single-Step Screening of the Potential Dependence of Metal Layer Morphologies along Bipolar Electrodes

Gwendoline Tisserant,[a, b] Julie Gillion,[a, b] Jérémy Lannelongue,[a, b] Zahra Fattah,[c] Patrick Garrigue,[a, b] Jérome Roche,[a, b] Dodzi Zigah,[a, b] Alexander Kuhn,[a, b] and Laurent Bouffier*[a, b]

The preparation of surface gradients is a hot topic in contemporary research. Among various physical chemistry approaches, bipolar electrochemistry allows the control of such gradients through the interfacial polarization between a conducting substrate and an electrolyte solution. Here, we report the straightforward, single-step generation of metal composition gradients on cylindrical carbon fibers. The screening of different metal deposit morphologies, which evolve gradually along a bipolar electrode, is demonstrated with monometallic layers as well as a bimetallic composite layer based on copper and nickel.

Bipolar electrochemistry (BPE) is an unconventional electrochemical approach, in which the driving force is imposed to the system by controlling the solution potential instead of the working-electrode potential.[1–4] Practically, two feeder electrodes are connected to an external power supply and immersed into an electrolyte solution. The application of an electric field across the solution results in an ohmic drop. When a conductive object is positioned in the field, an interfacial potential polarization appears and can ultimately promote electrochemical reactions at its extremities. The object behaves, therefore, as a bipolar electrode with an oxidation reaction taking place at the edge facing the feeder cathode, whereas a reduction process occurs at the side oriented towards the feeder anode.

BPE has, in fact, been known for a long time,[5, 6] but now encounters a true renewal, owing to new applications in the field of analytical science for the detection of (bio)molecules,[7–13] enrichment and separation of analytes,[14, 15] or screening of electroactive materials.[16–18] BPE also offers opportunities in materials science, because such an approach allows the direct electrochemical addressing of conducting objects in a wireless manner. The site-selective deposition of various types of layers at one extremity of a bipolar electrode has been exemplified with the reduction of metal salts,[19–22] the electrogeneration of organic polymers,[23] the electrografting of molecular layers,[24] and the deposition of inorganic species.[25–27] There are also several reports dealing with electroless deposition in bipolar cells.[28, 29]

By comparison to conventional interfacial methods that are often used to synthesize asymmetrically modified particles,[30] BPE can be used as a bulk approach, which promotes the simultaneous electrochemical modification of many discrete particles in a three-dimensional reaction space.[31, 32] Previously, BPE has been shown to be effective for designing surface gradients, as illustrated by the preparation of polymeric layers with doping gradients,[33–35] or molecular gradients that can be probed by heterogeneous electron transfer.[36, 37] Recently, metal-based gradients involving composition or roughness variation on planar bipolar surfaces have equally been described.[38–41] In the present Communication, the straightforward, single-step preparation of complex gradients exhibiting various metal morphologies on cylindrical bipolar electrodes is reported for the first time.
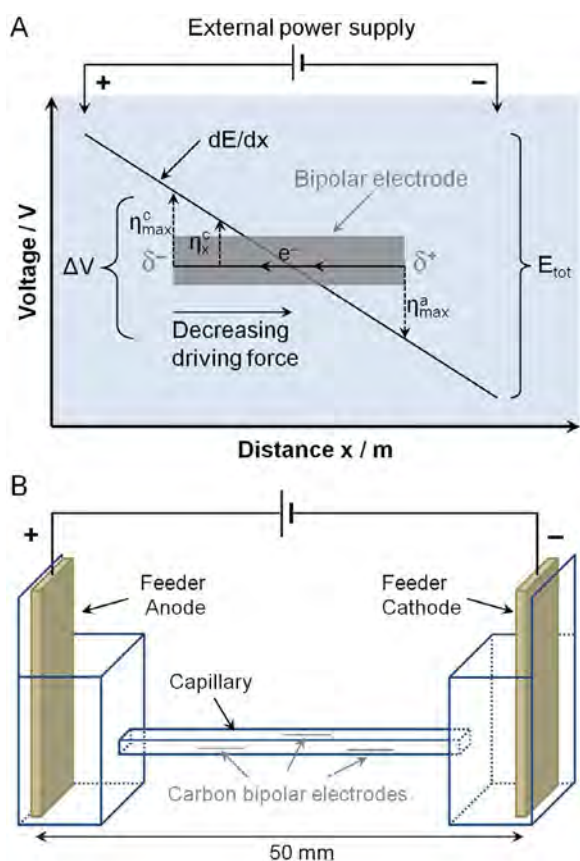
BPE is based on the electrochemical coupling of faradaic reactions across a bipolar electrode. The latter can be made from any sort of conducting or semiconducting material and is addressed electrochemically in a wireless fashion. The driving force is the interfacial polarization established between the electrolyte solution, where the electric field is applied, and the bipolar electrode, which behaves as an equipotential conductor. The maximum polarization potentials appear at the outermost edges of the bipolar electrode, whereas the electrochemical driving force decreases when moving towards the middle (Scheme 1 A). This point is crucial to achieve the fabrication of electrochemically driven gradients, because it implies that the thermodynamic and kinetic conditions of the redox process change alongside the bipolar electrode. The polarization is proportional to the electric-field strength and the length of the bipolar electrode, so that a typical polarization potential value (η_x) is associated with a position, x. The bipolar electrode can exhibit various geometries, and spherical glassy carbon beads or cylindrical carbon rods are often used.[19–21, 24–26] The longest symmetry axis of tubular substrates is aligned perpendicular to the feeder electrodes to follow the electric-field lines.[20] This is the reason why fibers, rather than beads, were chosen here in order to maintain a constant orientation. The used carbon

[a] G. Tisserant, J. Gillion, J. Lannelongue, P. Garrigue, Dr. J. Roche,
     Dr. D. Zigah, Prof. A. Kuhn, Dr. L. Bouffier
     University of Bordeaux
     Institute of Molecular Science (ISM), UMR 5255
     33400 Talence (France)
     E-mail: laurent.bouffier@enscbp.fr

[b] G. Tisserant, J. Gillion, J. Lannelongue, P. Garrigue, Dr. J. Roche,
     Dr. D. Zigah, Prof. A. Kuhn, Dr. L. Bouffier
     National Centre for Scientific Research (CNRS), ISM, UMR 5255
     33400 Talence (France)

[c] Dr. Z. Fattah
     University of Duhok
     Zakho Street 38, 1006 AJ Duhok
     Kurdistan Region (Iraq)
     An invited contribution to a Special Issue on Bipolar Electrochemistry

Scheme 1. Schematic representation of the promotion of faradaic reactions across a bipolar electrode (A) and the experimental setup for the modification of carbon fibers through bipolar electrodeposition (B).

ing that the interfacial polarization difference ΔV_{max}, established between the two ends of a bipolar electrode is, in a first approximation, a tenth of the potential difference applied by the external power supply (E_{tot}) [Eq. (1)]:

$$E_{tot}/d = \Delta V_{max}/l \tag{1}$$

where d is the distance between both feeder electrodes and l is the length of a bipolar microfiber.

Bipolar electrodeposition of copper was tested first. Such a metal is a good candidate for generating metal layer morphology gradients, because it is thermodynamically straightforward to reduce cationic precursors, and the conditions of deposition strongly affect the morphology.[42–44] Several experimental conditions were tested and a typical SEM image of a modified fiber is presented in Figure 1 B ($\times$200). This fiber was obtained by applying an electric field of 4 V cm^{-1} (i.e. $\Delta V_{max} \approx 2$ V) across an electrolyte solution containing 10 mM CuSO$_4$. The minimum polarization potential difference necessary to deposit Cu is given by the difference between the standard potentials of the two electrochemical reactions involved ($\Delta V_{min} = E^{\circ}_{O_2/H_2O} - E^{\circ}_{Cu^{2+}/Cu} = 1.23 - 0.34 = 0.89$ V). This means that the conditions used are favorable and the deposition is expected to occur not only at the extremity, but also along a large portion of the bipolar electrode. Experimentally, a long deposition zone was observed on the fiber ($\approx$ 700 μm) as well as a notable variation of the morphology. A selection of SEM images recorded with a higher magnification is shown as insets (Figure 1 B, $\times$1000). The latter clearly illustrates an evolution of the resulting Cu morphology from small and discrete clusters (for low η) to larger bundles and dendrites when moving towards the extremity of the bipolar electrode (high η). This can be explained by the thermodynamic and kinetic balance of the deposition, which varies from a slow nucleation and growth process to a faster growth regime.

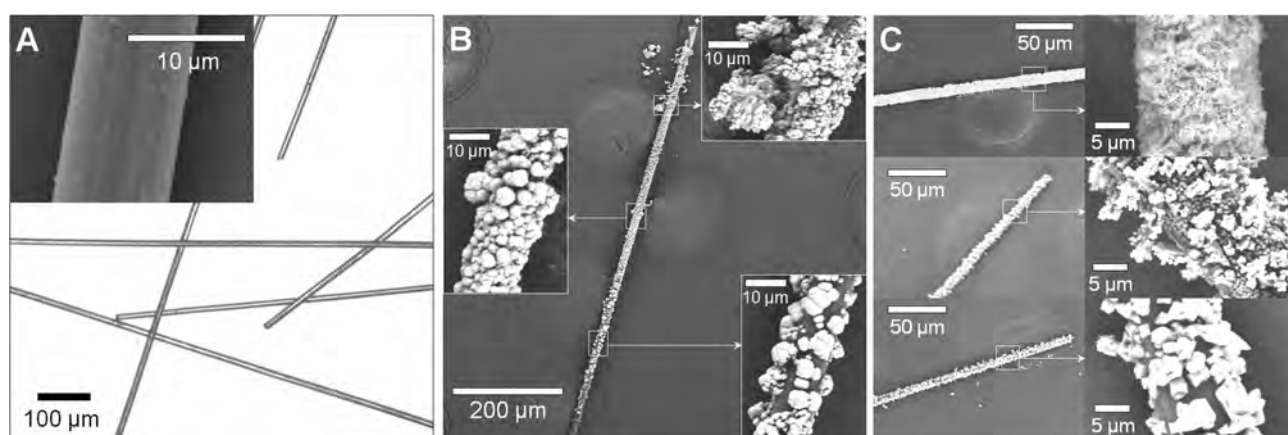To estimate the real experimental polarization reached during the BPE experiments, individual carbon fibers were also

fibers have a diameter of 10 μm, as shown in Figure 1 A. The BPE cell consists of two plastic reservoirs containing both feeder electrodes, which are connected by a glass capillary, in which the bipolar objects are positioned (Scheme 1 B). The feeder anode and cathode are separated by a distance of 5 cm, whereas the length of the carbon fibers is 5 mm, mean-

Figure 1. Optical image of carbon fibers (A) and a corresponding SEM image (inset). SEM images of a copper morphology gradient generated by using BPE when applying 4.0 V cm^{-1} for 15 min in a 10 mM CuSO$_4$ solution (B). SEM images of carbon fibers used as conventional electrodes for chronoamperometric copper deposition (C); $t = 15$ min, 1 mM CuSO$_4$ solution, and by applying from top to bottom $E = -0.30$ V, -0.20, and -0.15 V versus Ag/AgCl.

used as conventional electrodes. For that purpose, they were mounted on a glass substrate and wired by using conductive glue. Cu deposition was performed at various potential values by using chronoamperometry to compare the resulting morphologies (Figure 1 C). The SEM images recorded for applied potentials of −0.30, −0.20, and −0.15 V versus Ag/AgCl are presented from top to bottom. Low-magnification images on the left (×200) evidenced a uniform deposit along the fiber, as expected for conventional electrodeposition at a single thermodynamic condition. In the right-hand column, the high-magnification images (×3000) reveal the potential dependence of the metal morphology. The deposit at −0.15 V versus Ag/AgCl is composed of individual nucleation clusters that exhibit well-defined size and shape. In contrast, the Cu layer deposited at −0.30 V versus Ag/AgCl appears much thicker with a homogeneous entangled network. For the intermediate potential value (−0.20 V vs. Ag/AgCl), the SEM image shows a large number of clusters as well as bigger shapes that correspond to dendrites, which start to appear. Such a comparison demonstrates that the bipolar electrode was submitted to a whole range of different thermodynamic conditions in a single-step experiment. Moreover, the metal morphology gradient exhibits all the deposition regimes that were observed individually through conventional chronoamperometry.

In light of these encouraging results, the deposition of nickel was also performed. Ni^{II} salt reduction typically needs a higher driving force based on the difference of formal potential values ($\Delta V_{min} = E^{\circ}_{O_2/H_2O} - E^{\circ}_{Ni^{2+}/Ni} = 1.23 + 0.25 = 1.48$ V). Additionally, Ni^{II} reduction on carbon electrodes is associated with large overpotentials. In that case, the application of the same driving force that was previously used for Cu deposition would result in focusing the Ni on a smaller part of the bipolar electrode. Therefore, a higher electric field value of 6 V cm^{-1} (i.e. $\Delta V_{max} \approx 3$ V) was used instead in order to screen the Ni morphology on a significant length of the bipolar electrode. The corresponding modified carbon fibers exhibit a well-defined morphology gradient (Figure 2 A). The length of the observed Ni deposit is approximately 1150 μm (SEM, ×120). The beginning of the deposit, far from the edge of the fiber, appears as a thin metal layer with the presence of some clusters (×5000). Moving alongside the bipolar electrode towards its extremity reveals an evolution of the deposit, which becomes progressively thicker. Finally, near the outermost extremity, the Ni layer is even thicker and the larger amount of deposited metal results in several defects and cracks that allow an estimation of the layer thickness (ca. 2 μm).

A comparison with conventional electrodeposition was also carried out in the case of nickel, and these results are shown in Figure 2 B. Ni is more difficult to deposit than Cu and, therefore, a larger electrochemical window was selected (from top to bottom: $E = -0.50$, −1.00, and −1.20 V vs. Ag/AgCl). From the corresponding SEM images, it is clear that a potential value of −0.50 V versus Ag/AgCl is insufficient to promote Ni deposition (magnification of ×120 on the left and ×10000 on the right). The application of larger cathodic potential values of −1.00 or −1.20 V versus Ag/AgCl drives the metal deposition with an identical morphology to the one observed with BPE. In both cases, at −1.20 V, the Ni layer is homogeneous and very thick with tiny cracks starting to appear at −1.00 V as well as much deeper crevasses, revealing the carbon fiber underneath. These defects are large enough to affect the mechanical stability of the Ni layer, as observed for the fiber prepared by using BPE. This comparison reveals that the polarization experienced by the edge of the bipolar electrode was indeed superior to −1.00 V and, therefore, the simple observation of the morphology is a direct visualization of the polarization gradient.

After demonstrating the possibility to prepare Cu or Ni layers, independently, with a morphology gradient, a further step towards a more complex situation was made by performing the simultaneous co-deposition of the two metals. Such an approach was exemplified by mixing $CuSO_4$ and $NiSO_4$ precursors (1 mM for each). The BPE experiment was carried out by applying 4 V cm^{-1} for 30 min, as this driving force appears to be a good compromise for the simultaneous observation of both metal depositions. In fact, this value is large enough to drive Ni deposition on approximately 9% (i.e. 450 μm) of the
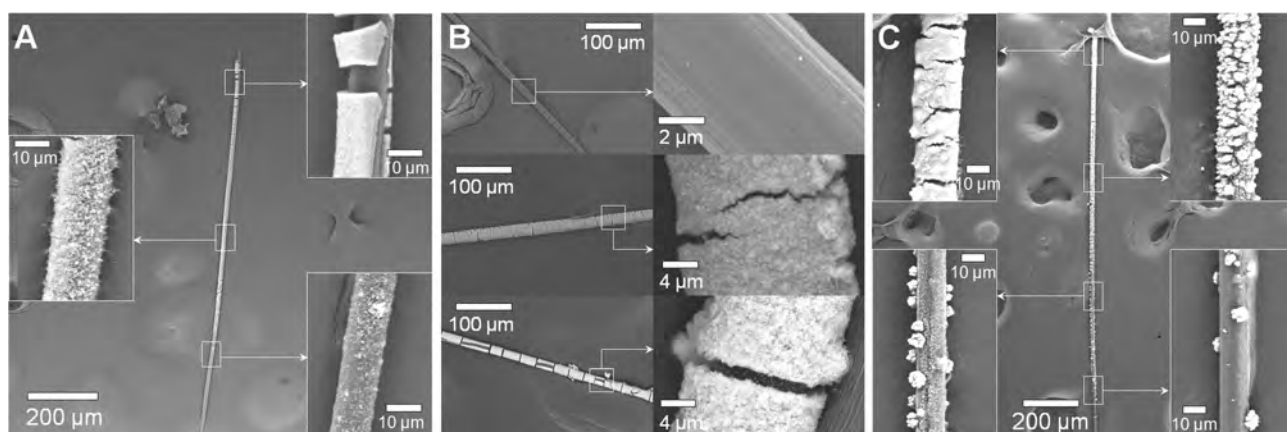

Figure 2. SEM images of a nickel morphology gradient generated through BPE when applying 6.0 V cm^{-1} for 15 min in a 1 mM NiSO$_4$ solution (A). SEM images of carbon fibers used as conventional electrodes for chronoamperometric nickel deposition (B); $t = 15$ min, 1 mM NiSO$_4$ solution, and by applying from top to bottom $E = -0.50$ V, −1.00, and −1.20 V versus Ag/AgCl. SEM images of a bimetallic Cu/Ni gradient generated through BPE when applying 4.0 V cm^{-1} for 30 min in a solution containing 1 mM of CuSO$_4$ and NiSO$_4$ (C).

carbon fiber, whereas larger electric-field values increase the Cu deposition rate too much to the detriment of good mechanical stability. Examination of the corresponding SEM images (Figure 2C, ×80 and ×1000) demonstrates the successful concomitant deposition of both metals. Also, the morphology of the co-deposit evolves from discrete Cu clusters to dendrites and bundles, with the extremity showing the combined signature of Cu (bundles) and Ni (thick layer) metals. One can note that the fibers used in this study are a good substrate to observe the morphology screening, but are also quite fragile and delicate to manipulate. This is the reason why the depositions were solely characterized with electronic microscopy. On the other hand, similar (co-)deposition experiments performed on planar gold surfaces and characterized through EDX analysis confirmed the chemical signature of Cu and Ni metals on the bipolar electrode.[41]

To conclude, BPE was advantageously used to prepare several metal layers, exhibiting a continuous variation of morphology alongside a carbon fiber that was used as the bipolar electrode. Two metals, namely copper and nickel, were used independently as a proof-of-principle of such an approach. The corresponding modified bipolar electrodes present features that are in good agreement with the variation of the thermodynamic conditions of the deposition at specific locations along the bipolar electrode. As a result, BPE allows simple and straightforward screening of the deposit morphology in one single step. The co-deposition of both metals was also tested and proved that a morphology gradient could be combined with a chemical composition gradient at the same time. It highlights that BPE could be an appropriate approach to study fundamental phenomena, such as metal electrodeposition, with the advantage of testing simultaneously multiple experimental conditions. Future applications of this screening method could lead to the simple identification of the most interesting metal morphology for specific spectroscopic (Raman or metal-enhanced fluorescence) or catalytic properties, which are sensitive to roughness factors.

Experimental Section

All chemicals were used as received, without further purification. Copper(II) sulfate (98%) was purchased from Alfa Aesar. Nickel(II) sulfate (>99.9%) and zinc(II) sulfate (>99.9%) were purchased from Sigma Aldrich. Solutions were prepared with Milli-Q water (resistivity = 18.2 MΩ cm^{-1}). Carbon fibers used as bipolar electrodes had a diameter of 10 μm and were cut to a length of 5 mm (Grade P100, Goodfellow).

Chronoamperometry was performed with a classic three-electrode setup (a carbon fiber as the working electrode, Pt grid as the auxiliary electrode, and Ag/AgCl as the reference electrode). The potential was applied by using a PGSTAT12 potentiostat from Autolab. The BPE cell was built with two standard disposable cuvettes purchased from VWR Jencons (external dimension: 12.5×12.5× 45 mm) acting as reservoirs and connected with a glass capillary (∅ = 1 mm). Feeder electrodes were glass surfaces (dimension 9× 25 mm) covered with a 360 nm-thick gold layer (ACM, France). During the BPE experiments, the electric field was applied with

a 6517B power supply from Keithley. Scanning electron microscopy (SEM) images were collected with a Hitachi microscope (TM-1000).

[1] F. Mavré, R. K. Anand, D. R. Laws, K.-F. Chow, B.-Y. Chang, J. A. Crooks, R. M. Crooks, *Anal. Chem.* **2010**, *82*, 8766–8774.
[2] G. Loget, A. Kuhn, *Anal. Bioanal. Chem.* **2011**, *400*, 1691–1704.
[3] S. E. Fosdick, K. N. Knust, K. Scida, R. M. Crooks, *Angew. Chem. Int. Ed.* **2013**, *52*, 10438–10456; *Angew. Chem.* **2013**, *125*, 10632–10651.
[4] G. Loget, D. Zigah, L. Bouffier, N. Sojic, A. Kuhn, *Acc. Chem. Res.* **2013**, *46*, 2513–2523.
[5] J. R. Backhurst, J. M. Coulson, F. Goodridge, R. E. Plimley, M. Fleischmann, *J. Electrochem. Soc. Electrochem. Technol.* **1969**, *116*, 1600–1607.
[6] M. Fleischmann, J. Ghoroghchian, D. Rolison, S. Pons, *J. Phys. Chem.* **1986**, *90*, 6392–6400.
[7] K.-F. Chow, F. Mavré, R. M. Crooks, *J. Am. Chem. Soc.* **2008**, *130*, 7544–7545.
[8] K.-F. Chow, B.-Y. Chang, B. A. Zaccheo, F. Mavré, R. M. Crooks, *J. Am. Chem. Soc.* **2010**, *132*, 9228–9229.
[9] T. Wang, S. Fan, R. Erdmann, C. Shannon, *Langmuir* **2013**, *29*, 16040–16044.
[10] M.-S. Wu, G.-s. Qian, J.-J. Xu, H.-Y. Chen, *Anal. Chem.* **2012**, *84*, 5407–5414.
[11] Q.-M. Feng, J.-B. Pan, H.-R. Zhang, J.-J. Xu, H.-Y. Chen, *Chem. Commun.* **2014**, *50*, 10949–10951.
[12] L. Bouffier, T. Doneux, B. Goudeau, A. Kuhn, *Anal. Chem.* **2014**, *86*, 3708–3711.
[13] V. Eßmann, D. Jambrec, A. Kuhn, W. Schuhmann, *Electrochem. Commun.* **2015**, *50*, 77–80.
[14] D. R. Laws, D. Hlushkou, R. K. Perdue, U. Tallarek, R. M. Crooks, *Anal. Chem.* **2009**, *81*, 8923–8929.
[15] K. N. Knust, E. Sheridan, R. K. Anand, R. M. Crooks, *Lab Chip* **2012**, *12*, 4107–4114.
[16] S. E. Fosdick, S. P. Berglund, C. B. Mullins, R. M. Crooks, *Anal. Chem.* **2013**, *85*, 2493–2499.
[17] X. Lin, L. Zheng, G. Gao, Y. Chi, G. Chen, *Anal. Chem.* **2012**, *84*, 7700–7707.
[18] G. Loget, S. So, R. Hahn, P. Schmuki, *J. Mater. Chem. A* **2014**, *2*, 17740–17745.
[19] Z. Fattah, G. Loget, V. Lapeyre, P. Garrigue, C. Warakulwit, J. Limtrakul, L. Bouffier, A. Kuhn, *Electrochim. Acta* **2011**, *56*, 10562–10566.
[20] Z. Fattah, P. Garrigue, V. Lapeyre, A. Kuhn, L. Bouffier, *J. Phys. Chem. C* **2012**, *116*, 22021–22027.
[21] Z. Fattah, P. Garrigue, B. Goudeau, V. Lapeyre, A. Kuhn, L. Bouffier, *Electrophoresis* **2013**, *34*, 1985–1990.
[22] T. M. Braun, D. T. Schwartz, *J. Electrochem. Soc.* **2015**, *162*, D180–D185.
[23] T. Kuwahara, K. Sato, M. Kondo, M. Shimomura, *Synth. Met.* **2014**, *198*, 274–276.
[24] W. Kumsapaya, M.-F. Bakai, G. Loget, B. Goudeau, C. Warakulwit, J. Limtrakul, A. Kuhn, D. Zigah, *Chem. Eur. J.* **2013**, *19*, 1577–1580.
[25] G. Loget, J. Roche, E. Gianessi, L. Bouffier, A. Kuhn, *J. Am. Chem. Soc.* **2012**, *134*, 20033–20036.
[26] Z. Fattah, J. Roche, P. Garrigue, D. Zigah, L. Bouffier, A. Kuhn, *ChemPhysChem* **2013**, *14*, 2089–2093.
[27] S. Yadnum, J. Roche, E. Lebraud, P. Négrier, P. Garrigue, D. Bradshaw, C. Warakulwit, J. Limtrakul, A. Kuhn, *Angew. Chem. Int. Ed.* **2014**, *53*, 4001–4005; *Angew. Chem.* **2014**, *126*, 4082–4086.
[28] D. Plana, G. Shul, M. J. Stephenson, R. A. W. Dryfe, *Electrochem. Commun.* **2009**, *11*, 61–64.
[29] D. Plana, R. A. W. Dryfe, *Electrochem. Commun.* **2013**, *37*, 8–10.
[30] G. Loget, A. Kuhn, *J. Mater. Chem.* **2012**, *22*, 15457–15474.
[31] G. Loget, J. Roche, A. Kuhn, *Adv. Mater.* **2012**, *24*, 5111–5116.
[32] J. Roche, G. Loget, D. Zigah, Z. Fattah, B. Goudeau, S. Arbault, L. Bouffier, A. Kuhn, *Chem. Sci.* **2014**, *5*, 1961–1966.
[33] S. Inagi, Y. Ishiguro, M. Atobe, T. Fuchigami, *Angew. Chem. Int. Ed.* **2010**, *49*, 10136–10139; *Angew. Chem.* **2010**, *122*, 10334–10337.
[34] Y. Ishiguro, S. Inagi, T. Fuchigami, *Langmuir* **2011**, *27*, 7158–7162.

[35] S. Inagi, H. Nagai, I. Tomita, T. Fuchigami, *Angew. Chem. Int. Ed.* **2013**, *52*, 6616 – 6619; *Angew. Chem.* **2013**, *125*, 6748 – 6751.

[36] C. Ulrich, O. Andersson, L. Nyholm, F. Björefors, *Angew. Chem. Int. Ed.* **2008**, *47*, 3034 – 3036; *Angew. Chem.* **2008**, *120*, 3076 – 3078.

[37] C. Ulrich, O. Andersson, L. Nyholm, F. Björefors, *Anal. Chem.* **2009**, *81*, 453 – 459.

[38] R. Ramaswamy, C. Shannon, *Langmuir* **2011**, *27*, 878 – 881.

[39] S. Ramakrishnan, C. Shannon, *Langmuir* **2010**, *26*, 4602 – 4606.

[40] N. Dorri, P. Shahbazi, A. Kiani, *Langmuir* **2014**, *30*, 1376 – 1382.

[41] G. Tisserant, Z. Fattah, C. Ayela, J. Roche, B. Plano, D. Zigah, B. Goudeau, A. Kuhn, L. Bouffier, *Electrochim. Acta* **2015**, DOI: 10.1016/j.electacta.2015.03.102.

[42] N. D. Nikolić, K. I. Popov, Lj. J. Pavlović, M. G. Pavlović, *J. Electroanal. Chem.* **2006**, *588*, 88 – 98.

[43] A. Radisic, P. M. Vereecken, P. C. Searson, F. M. Ross, *Surf. Sci.* **2006**, *600*, 1817 – 1826.

[44] S. Song, C. M. Ortega, Z. Liu, J. Du, X. Wu, Z. Cai, L. Sun, *J. Electroanal. Chem.* **2013**, *690*, 53 – 59.